

Typhoon-driven variations in primary production and phytoplankton assemblages in Sagami Bay, Japan: A case study of typhoon *Mawar* (T0511)

KENJI TSUCHIYA^{1,*}, TOMOKO YOSHIKI², RYOTA NAKAJIMA^{1,3}, HIDEO MIYAGUCHI^{1,5}, VICTOR S. KUWAHARA¹, SATORU TAGUCHI¹, TOMOHIKO KIKUCHI⁴ & TATSUKI TODA¹

¹ Graduate School of Engineering, Soka University, 1–236 Tangi-cho, Hachioji, Tokyo 192–8577, Japan

² National Research Institute of Fisheries Science, Fisheries Research Agency, 2–12–4 Fukuura, Kanazawa, Yokohama, Kanagawa 236–8648, Japan

³ Japan Agency for Marine–Earth Science and Technology, 2–15 Natsushima-cho, Yokosuka, Kanagawa 237–0061, Japan

⁴ Graduate School of Environment and Information Science, Yokohama National University, 79–7 Tokiwadai, Hodogaya-ku, Yokohama, Kanagawa 240–8501, Japan

⁵ Present address: House of Representatives, 2nd Members' Office Building, 2–1–2 Nagata-cho, Chiyoda-ku, Tokyo 100–8982, Japan

Received 13 June 2012; Accepted 11 April 2013

Abstract: Climate change has the potential for intensification of typhoons, which will cause stronger effects on aquatic ecosystems in the future. The effect of typhoon *Mawar* (T0511), passing Manazuru Port located in the western part of Sagami Bay, Japan, was investigated from August to September 2005. Immediately after the passage of *Mawar*, photosynthetically available radiation showed high values, salinity decreased dramatically and nutrient concentrations (NO_2+NO_3 , PO_4 and $\text{Si}(\text{OH})_4$) increased. *Skeletonema* spp. and *Leptocylindrus* spp. were dominant after the passage of *Mawar*, and their succession was linked to the variability of the N/P ratio. Primary production was highest at $349 \text{ mg C m}^{-3} \text{ day}^{-1}$ three days after *Mawar*, and high assimilation numbers lasted for nine days. The integrated primary production during the nine days after *Mawar* was $2.1 \times 10^3 \text{ mg C m}^{-3}$, which accounted for 7.2–9.1% of the annual primary production in the upper waters of Sagami Bay. The study confirms that enhanced primary production induced by episodic typhoon events in temperate coastal regions are significant, and should be considered in annual primary production estimates.

Key words: typhoon, phytoplankton, primary production, temperate coastal water

Introduction

As the reality of climate change and global warming has become more apparent, the intensity of typhoons, tropical cyclones, and hurricanes has increased (Emanuel 2005, Webster et al. 2005, Elsner et al. 2008, Yamada et al. 2010). The destructiveness of typhoons has increased over the past 30 years, showing high correlation with rising sea surface temperatures (Emanuel 2005). The intensity of the strongest types of typhoons has increased (Elsner et al. 2008). A simulation using a global cloud-system-resolving model (GCRM) predicted increases in the frequency of the more intense typhoons with global warming (Yamada

et al. 2010). Based on these studies, it is conceivable that intensification of typhoons will cause stronger physical disturbances in aquatic ecosystems.

Strong wind and heavy rain accompanied by typhoon passage induce physical disturbances such as upwelling and vertical mixing (Price 1981, Lin et al. 2003, Zheng & Tang 2007), terrestrial runoff (Zheng & Tang 2007, Chen et al. 2009) and sediment resuspension (Fogel et al. 1999), which supplies nutrients to the photic layer (e.g. Shiah et al. 2000). Consequently, phytoplankton biomass and production increase significantly (e.g. Lin et al. 2003, Chen et al. 2009; Table 1). Contribution of the increased primary production to annual primary production has primarily been estimated in tropical and subtropical regions. In the oligotrophic South China Sea, Lin et al. (2003) observed

* Corresponding author: Kenji Tsuchiya; E-mail, ktsuchiya@soka.gr.jp

Table 1. Summary of chlorophyll *a* (Chl *a*) concentration and primary production before and after typhoon passages.

Study site	Name of typhoon*	Chl <i>a</i> (mg m ⁻³)			Primary production			Reference
		Before (B)	After (A)	A/B	Before (B)	After (A)	A/B	
mg C m ⁻² d ⁻¹								
Oceanic								
South China Sea	<i>Kai-Tak</i>	0.10	3.2	32	3.0 × 10 ²	2.8 × 10 ³	9.3	Lin et al. 2003
South China Sea	<i>Ling-Ling</i>	0.14	0.45	3.2	2.7 × 10 ²	2.6 × 10 ³	9.6	Zhao et al. 2008
South China Sea	<i>Kai-Tak</i>	0.15	0.56	3.7	3.1 × 10 ²	4.1 × 10 ³	13	Zhao et al. 2008
South China Sea	<i>Hagibis</i>	0.14	0.74	5.3				Sun et al. 2010
mg C m ⁻³ d ⁻¹								
Coastal								
North Carolina	<i>Gordon</i>	0.56	1.1	2.0				Fogel et al. 1999
Gulf of Mexico**	<i>Ivan</i>	0.24–0.36	0.81–0.99	2.3–4.1				Walker et al. 2005
South China Sea	<i>Damrey</i>	0.15	0.72	4.8				Zheng & Tang 2007
Philippine Sea**	<i>Pabuk, Wutip, Sepat</i>	0.06–0.11	0.22–0.56	2.0–5.6	7.6–8.0	12–76	1.5–10	Chen et al. 2009
South Carolina**	<i>Dennis</i>	1.0–11	2.5–6.0	0.56–2.58	0.13–2.1 × 10 ³	0.83–2.5 × 10 ³	1.2–6.3	Zeeman 1985
the Reef of Tiafura	<i>Wasa</i>	0.12	0.21	1.8	9.1	14	1.5	Delesalle et al. 1993
Northern Taiwan	<i>Tim</i>	0.40–1.8	4.2	2.3–11				Chang et al. 1996
Northern Taiwan	<i>Caitlin, Doug</i>	0.30	3.5	12				Chang et al. 1996
Northern Taiwan	<i>Fred</i>	0.60	2.0	3.3				Chang et al. 1996
North Carolina**	<i>Gordon</i>	0.56	0.56–3.4	1.0–6.0	18	53	2.9	Fogel et al. 1999
Taiwan Strait**	<i>Herb</i>	0.28–0.48	0.42–0.91	0.89–2.1	2.2–2.6	10–50	3.9–19	Shiah et al. 2000
Sagami Bay	<i>Mawar</i>	2.6	7.8	3.0	80***	3.5 × 10 ²	4.4	Present study

*Typhoon in the table includes tropical cyclones and hurricanes

**Ranges of data are based on individual calculations from multiple sampling stations

***Primary production before *Mawar* was the mean value in summer at Sta. A derived from Satoh et al. (2000)

chlorophyll *a* (chl *a*) concentrations before and after the passage of typhoon *Kai-Tak* using three remote sensing observational platforms (SeaWiFS, TRMM and QuickSCAT), estimated primary production using a vertical generalized production model algorithm (VGPM; Behrenfeld & Falkowski 1997), and reported that the estimated primary production resulting from the typhoon alone contributed at least 2–4% to the annual new production. Given an annual average of fourteen typhoons passing over the South China Sea, the contribution of typhoons to the South China Sea's annual new production may be as much as 20–30% (Lin et al. 2003). Although typhoons are episodic events, the effect of a typhoon on lower trophic production, such as primary production, is significant, and should be considered in annual primary production estimates. Temperate coastal regions play an important role in the global carbon cycle due to their high primary productivity and high contribution to new production (Paerl 1995, Jickells 1998). However, information is still limited with regards to quantitative estimates of primary production contributions to the annual primary production during typhoons.

Recent studies have revealed some noticeable effects of typhoon disturbances on coastal pelagic communities. Some studies showed diatoms such as *Skeletonema* spp., *Chaetoceros* spp. and *Nitzschia* spp. often dominated phytoplankton assemblages after typhoon passages in various regions (e.g. Glynn et al. 1964, Zeeman 1985, Furnas 1989,

Chang et al. 1996, Chen et al. 2009). Dominance of diatoms after typhoon passage might be attributed to their high growth rate (Furnas 1990), which should contribute to increases in the sinking flux of carbon (Chen et al. 2009). Phytoplankton successions are known to be linked to and regulated by nutrients (e.g. Escaravage et al. 1996, Estrada et al. 2003, Lagus et al. 2004). However, the succession process of phytoplankton community structures, and their relationship to nutrient stoichiometry after typhoon passage are still relatively unknown.

Sagami Bay, located in the central part of Japan (Fig. 1), is considered one of the key representative bays for temperate areas because the physical, chemical and biological environments have been comprehensively investigated by many authors over a long period (e.g. Ogura 1975, Hogetsu & Taga 1977, Horikoshi 1977, Nakata 1985, Kitazato et al. 2000, Kuwahara et al. 2000a, b, Kanda et al. 2003, Fujiki et al. 2004, Hashimoto et al. 2005, Miyaguchi et al. 2008, Ara & Hiromi 2009, Ara et al. 2011). Twenty rivers including two large rivers (Sakawa River and Sagami River) flow into the bay (Hirano 1969), which leads to the formation of low salinity water masses in nearshore areas. One of the areas influenced is the western, nearshore part of Sagami Bay, including Manazuru Port. A prior study of the primary production in the area reported an annual production of 2.9 × 10⁴ mg C m⁻³ yr⁻¹ (Satoh et al. 2000). During the study, a summer phytoplankton bloom occurred after 3–4

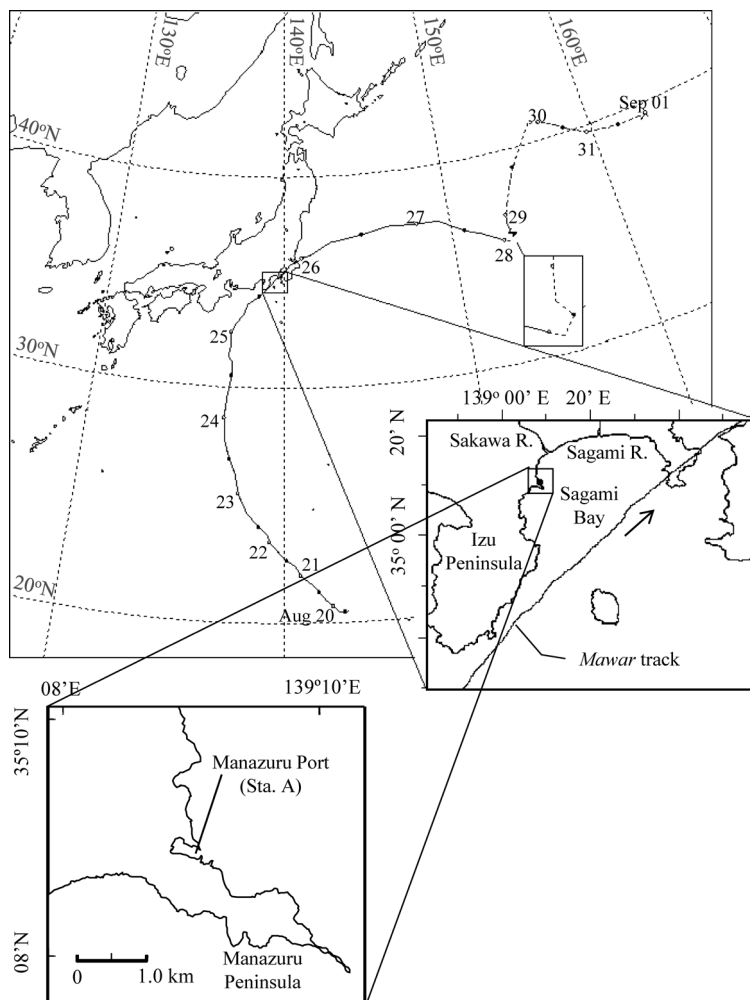


Fig. 1. Track of typhoon *Mawar* (T0511) and the location of Manazuru Port (Sta. A) in Sagami Bay, Japan. Open and closed circles describe 9:00 and 21:00, respectively. Solid and dashed lines of track describe typhoon and extra-tropical cyclone, respectively. Typhoon *Mawar* passed Sagami Bay at 2:00 on Day 0 (26 August 2005).

days of persistent precipitation of 200 mm or more, and the bloom was dominated by large-sized dinoflagellates, such as *Ceratium furca* Ehrenberg (Sato et al. 2000). Increase in freshwater discharge due to precipitation results in large loadings of nitrogen and silicate to the coastal area, which leads to phosphorus limitation of primary productivity from spring to summer (Fujiki et al. 2004, Baek et al. 2009). Although variability in phytoplankton communities and primary production has been documented in the near-shore, western part of Sagami Bay, information on the importance of episodic events remains limited.

The present study examines the influence of the passage of a strong typhoon on lower trophic levels in the coastal waters of Sagami Bay by conducting a time-series observation during the passage of typhoon *Mawar* (T0511) in August 2005. The specific objectives of the study were to clarify the pre- and post- effects of *Mawar* on the physical and chemical environments, and to quantify primary production and phytoplankton succession using bi-daily sam-

pling in order to detect quick responses.

Materials and Methods

Typhoon *Mawar*

Typhoon *Mawar* (T0511) emerged near the Ogasawara Islands in southern Japan as a tropical depression on 20 August 2005 (Japan Meteorological Agency, <http://www.jma.go.jp/jp/typh/>; Fig. 1). *Mawar* then moved northward and its track changed northward with an average speed of 16.3 km h^{-1} . At 2:00 on 26 August, *Mawar* entered Sagami Bay. *Mawar*'s 260 km diameter area of storm force winds coincided with heavy precipitation and storm conditions around central Japan. The lowest sea-level pressure of *Mawar* was 930 hPa and the maximum wind speed recorded was approximately 50 m sec^{-1} . *Mawar* passed through Sagami Bay, and was downgraded to an extra-tropical cyclone on 28 August 2005 off the east coast of

Honshu Island, Japan. Data on *Mawar* were obtained from the Japan Meteorological Agency.

Sampling procedures

Sampling was conducted at Sta. A located at the mouth of Manazuru Port (35°09'49"N, 139°10'33"E, maximum depth 5 m; Fig. 1) in Sagami Bay, Japan, from 23 August to 8 September 2005, which included the time period before and after the passage of typhoon *Mawar*. In this study, we defined the day *Mawar* passed Sta. A as Day 0 (i.e. 0:00 on 26 August 2005) while 25 and 27 August 2005 were defined as Day -1 and Day 1, respectively.

Surface seawater samples were collected every 12 hrs at 0:00 and 12:00 during the study period, and analyzed for water temperature, salinity, inorganic macronutrients (NO_2+NO_3 , PO_4 and $\text{Si}(\text{OH})_4$), chl *a* and particulate organic carbon (POC) concentrations. Instrument precision of the refractometer for salinity measurement (ATAGO Co., Ltd.) used in the present study was $\pm 2\%$. We also collected samples for study of the phytoplankton assemblages every 24 hrs (0:00). Primary production measurements were conducted every 2 d after Day 1. The sampling at 0:00 on Day 0 was interrupted because *Mawar* was closest to the sampling site. The seawater sample collected at 12:00 on Day 0 was used for the phytoplankton assemblage sample of Day 0. Collected water samples were pre-screened through 180 μm nylon mesh to remove large zooplankton and debris, and were immediately brought back to the field laboratory (Manazuru Marine Center for Environmental Research and Education, Yokohama National University).

Triplicate subsamples for inorganic macronutrient analyses were filtered through a 0.45 μm pore size (Millex SLHA, Millipore) membrane filter, placed into 10 mL plastic tubes, and stored at -20°C until analysis. The concentrations of NO_2+NO_3 , PO_4 and $\text{Si}(\text{OH})_4$ were measured as described by Parsons et al. (1984) using a nutrient auto-analyzer (AACS-II, Bran + Luebbe).

Duplicate subsamples of 300 to 500 mL for POC measurement were filtered onto pre-combusted (450°C, 4 h) glass fiber filters (GF/F, Whatman). The filters were treated with HCl fumes for 2 h to remove inorganic carbon, dried at 60°C for 12 h in a dry oven, and stored in a desiccator until analysis. POC concentration was determined using an elemental analyzer (Instruments NA-1500 CNS, FISON) according to Nagao et al. (2001).

Subsamples for chl *a* analysis were filtered onto a 10 μm membrane filter (JCWP, Millipore), then the filtrate was filtered through a 2 μm membrane filter (TTTP, Millipore) before finally being filtered through a 0.2 μm membrane filter (JGWP, Millipore). These three size fractions of 10–180 μm , 2–10 μm and 0.2–2 μm were defined as microplankton, nanoplankton and picoplankton, respectively (Sieburth et al. 1978). The filters were immersed in *N,N*-dimethylformamide (DMF) and stored at 4°C for 24 h (Suzuki & Ishimaru 1990). Chl *a* concentration was deter-

mined fluorometrically (Model 10-AU, Turner Design) according to Holm-Hansen et al. (1965).

Primary production was measured using the stable isotope ^{13}C (Hama et al. 1983). Subsamples collected from the surface water at 9:00 were dispensed into acid washed 4 L polycarbonate bottles (two light bottles and one dark bottle), and were incubated *in situ* for 24 h after the addition of ^{13}C -sodium bicarbonate (final ^{13}C atom% of total dissolved inorganic carbon was $\sim 10\%$ of that in the ambient water; Hama et al. 1983). After incubation, duplicate aliquots of 200 mL were filtered onto pre-combusted (450°C, 4 h) glass fiber filters (GF/F, Whatman) to determine the bulk carbon fixation rate. The filters were treated using the same procedure as for the POC measurements described above. The concentration of POC and the isotopic ratios of ^{13}C and ^{12}C were determined by a mass spectrometer (TracerMat, Finnigan MAT) combined with an elemental analyzer (Instruments NA-1500 CNS, Fisions). Primary production of phytoplankton was calculated according to Hama et al. (1983). In the present study, dissolved inorganic carbon (DIC) was not measured, and primary production was calculated assuming $\text{DIC}=2.2\text{ mM}$ (Gao & McKinley 1994). The dark uptake was always corrected for primary production. In order to calculate the amount of carbon fixed per unit of chlorophyll *a* per day, the assimilation number, chl *a* concentration was measured as described above.

Samples for phytoplankton taxonomic identification (500 mL) were fixed in a 2% glutaraldehyde solution. Five to 20 mL of the phytoplankton sample was poured into a settling chamber (HYDRO-BIOS), and settled for 24 h (Hasle 1978). Identification and enumeration of microphytoplankton species, especially diatoms and dinoflagellates, was conducted using an inverted microscope (Axiovert 25, Carl Zeiss) according to Fukuyo et al. (1990) and Chihara et al. (1997) for dinoflagellates, and Hasle & Syvertsen (1997) for diatoms. More than 400 phytoplankton cells were counted per sample. Other phytoplankton taxa were excluded from the analysis due to low abundance. The taxonomic composition of microphytoplankton was analyzed by the multidimensional scaling (MDS) method using the Bray-Curtis similarity index in order to examine the dynamics of the phytoplankton community structure.

Meteorological data

Atmospheric pressure, wind speed, wind direction and precipitation data were obtained from the Japan Meteorological Agency (<http://www.jma.go.jp/>) at the Ajiro Office, Shizuoka, Japan (35°02.7'N, 139°05.5'E), which is located on the east coast of the Izu Peninsula and less than 15 km away from our sampling site. Atmospheric pressure, wind speed and wind direction are mean values per hour. Precipitation is shown as daily integrated values. Photosynthetically active radiation (PAR) was measured every day during the study period with a surface radiometer (LI-190 SA, LI-COR) placed on the roof of the Manazuru field labora-

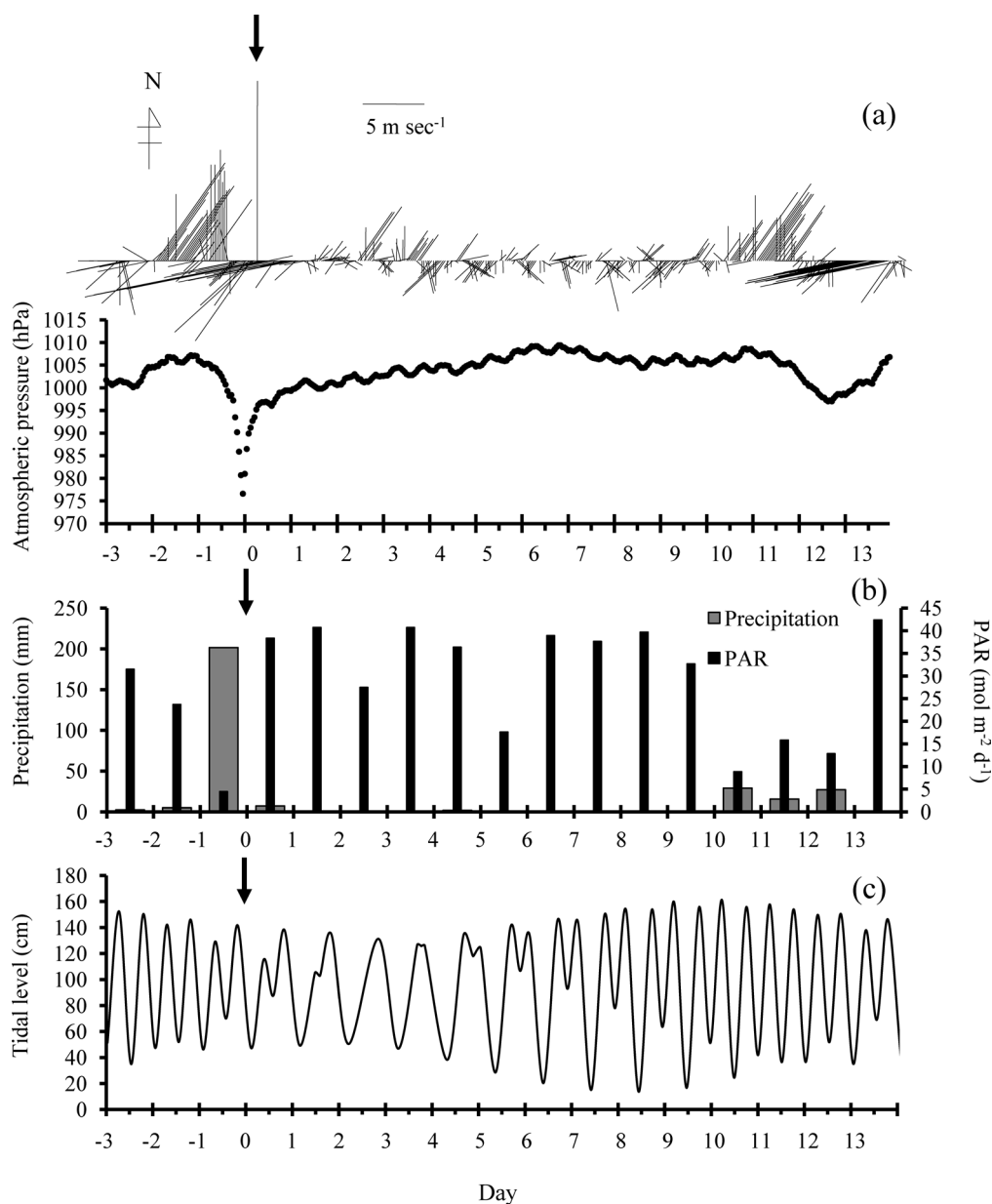


Fig. 2. Temporal variations in meteorology as (a) wind stick diagram and atmospheric pressure, (b) precipitation and photo-synthetically active radiation (PAR) and (c) tidal level. Arrows show the day of the passage of typhoon *Mawar* in Sagami Bay, Japan.

tory. PAR is shown as daily integrated values. Tidal level at Manazuru Port was obtained by calculation based on the tidal harmonic constants tables (Hydrographic Department, Japan Coast Guard 1992).

Results

Meteorological, physical and chemical environments

Atmospheric pressure declined suddenly during the passage of *Mawar*, and the minimum value of 977 hPa was recorded on Day 0 (Fig. 2a). Before *Mawar*, from Day -2 to

Day -1, relatively high wind speed was observed, reaching a maximum of 14.6 m sec⁻¹ on Day 0. During the passage of *Mawar*, the wind direction was west-southwest. The maximum daily precipitation of 202 mm and the minimum PAR of 4.5 mol m⁻² d⁻¹ was recorded on Day -1 (Fig. 2b). It did not rain after the passage of *Mawar* for nine days, and the average irradiance was 35.3 mol m⁻² d⁻¹. From Day 10 to Day 12, the PAR showed relatively low values. After Day 5, middle and spring tides were observed, and between Day 5 and Day 8 strong ebb tides occurred (Fig. 2c). Water temperature rose up from 25.5 (Day -0.5) to 27.0°C (Day 0.5) with the passage of *Mawar* (Fig. 3a).

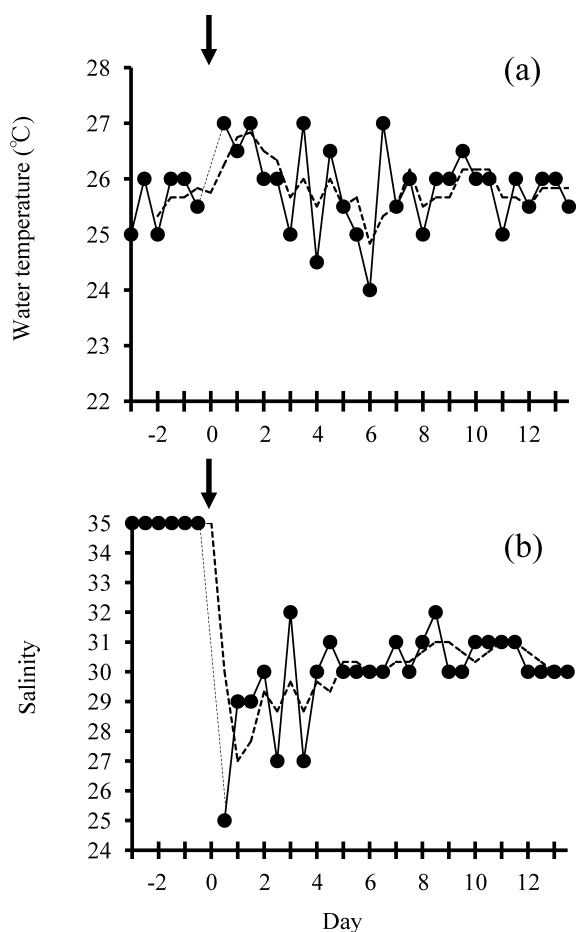


Fig. 3. Temporal variations in (a) water temperature and (b) salinity at the surface at Sta. A. Arrows show the day of the passage of typhoon *Mawar* in Sagami Bay, Japan. The sampling at 0:00 on Day 0 was interrupted because *Mawar* was closest to the sampling site (dashed line). The dotted lines indicate three-point moving averages.

Water temperature generally declined to 24.0°C until Day 6. Salinity declined significantly from 35 to 25 during the passage of *Mawar* (Fig. 3b). Salinity stabilized at around 30.5 ± 0.6 on average from Day 4 to the end of the study period.

After *Mawar* passed (Day 1 to Day 2), the concentration of $\text{NO}_2 + \text{NO}_3$ increased 3 times compared with that before *Mawar* ($5.9 \pm 1.6 \mu\text{M}$ on average from Day -3 to Day -0.5), and reached a maximum of $17.8 \pm 1.3 \mu\text{M}$ on Day 2 (Fig. 4a). Thereafter, the concentration returned to similar levels ($7.4 \pm 3.0 \mu\text{M}$ on average from Day 5 to Day 13.5) as to that before the passage of *Mawar* (Student's *t*-test, $p > 0.05$). The concentration of PO_4 increased from $0.35 \pm 0.01 \mu\text{M}$ on Day -2 to $1.22 \pm 0.22 \mu\text{M}$ on Day -0.5 (Fig. 4b). The maximum value of $1.54 \pm 0.01 \mu\text{M}$ was observed on Day 2, and then decreased to a minimum of $0.13 \pm 0.01 \mu\text{M}$ on Day 9.5. The concentration of $\text{Si}(\text{OH})_4$ increased from $12.4 \pm 6.2 \mu\text{M}$ on Day -2 to $76.5 \pm 2.2 \mu\text{M}$ on Day 2.5 (up to 6.2 times)

after the passage of *Mawar* (Fig. 4c). Relatively high concentrations of $\text{Si}(\text{OH})_4$ ($59.0 \pm 11.8 \mu\text{M}$ on average from Day 0.5 to Day 7) lasted until Day 7, before the concentration decreased in general, and returned to similar levels as to prior to the passage of *Mawar*. The N/P ratio exhibited a mean of 7.46 ± 1.40 before the passage of *Mawar* (Fig. 4d), before increasing to a mean of 13.5 ± 1.4 by Day 3. After Day 9, the N/P ratio fluctuated within relatively high values (29.6 ± 7.8 , from Day 9 to Day 13). There were significant inverse relationships between the concentrations of $\text{NO}_2 + \text{NO}_3$ and $\text{Si}(\text{OH})_4$, and salinity (Pearson's correlation coefficient test, $p < 0.001$; Fig. 5a, c). No significant relationship was observed between salinity and PO_4 concentration (Fig. 5b).

POC, Chl *a* and primary production

The POC concentration increased from 246 mg m^{-3} on Day -3 to 480 mg m^{-3} on Day -0.5 (Fig. 6a) and abruptly declined on Day 0.5, remaining low until Day 3 ($225 \pm 39 \text{ mg m}^{-3}$ on average). The POC concentration increased abruptly again to a maximum of 556 mg m^{-3} on Day 4.

Time-series variability of total chl *a* concentration (sum of each fraction) was similar to that of POC concentration, except for the peak of POC before the passage of *Mawar* (Fig. 6b). The mean concentration of total chl *a* was $2.60 \pm 1.22 \text{ mg m}^{-3}$ before *Mawar* (from Day -3 to Day -0.5; Fig. 6b). Just after *Mawar*, chl *a* concentrations decreased to 0.51 mg m^{-3} on Day 0.5, and then abruptly increased, exhibiting the highest value of 7.84 mg m^{-3} on Day 5. Another chl *a* peak (4.14 mg m^{-3}) was observed on Day 9.5, and then concentrations declined and returned to the values prevalent before the passage of *Mawar*. Chl *a* concentrations of the microplankton (10–180 μm), nanoplankton (2–10 μm) and picoplankton (0.2–2 μm) fraction occupied $72.2 \pm 9.1\%$, $23.1 \pm 7.2\%$ and $4.7 \pm 5.4\%$ of the total on average, respectively, before the passage of *Mawar* (Fig. 6b). After *Mawar*, the mean relative contributions of microplankton, nanoplankton and picoplankton were $61.1 \pm 12.1\%$, $27.1 \pm 10.0\%$ and $11.8 \pm 9.6\%$, respectively. Both before and after the passage of *Mawar*, the proportion of the microplankton fraction was significantly higher than the values of the other two fractions (Scheffé's *F* multiple comparison, $p < 0.01$). The variation in the microplankton fraction concentration explained 94% ($R^2 = 0.935$, $n = 33$) of the variation in total chl *a* concentration.

Sea surface primary production was $81.3 \text{ mg C m}^{-3} \text{ d}^{-1}$ (Fig. 6c) on Day 1, just after the passage of *Mawar*. The highest value of $349 \text{ mg C m}^{-3} \text{ d}^{-1}$ was reached on Day 3. After that, primary production was relatively high until Day 9, then decreased abruptly from Day 11. The amount of carbon fixed per unit of chlorophyll *a* per day, the assimilation number, exhibited relatively high values from Day 1 to Day 9 ($131 \text{ mg C [mg Chl } a]^{-1} \text{ d}^{-1}$; Fig. 6d), and relatively low values were observed (22 and $38 \text{ mg C [mg Chl } a]^{-1} \text{ d}^{-1}$; Fig. 6d) from Day 11.

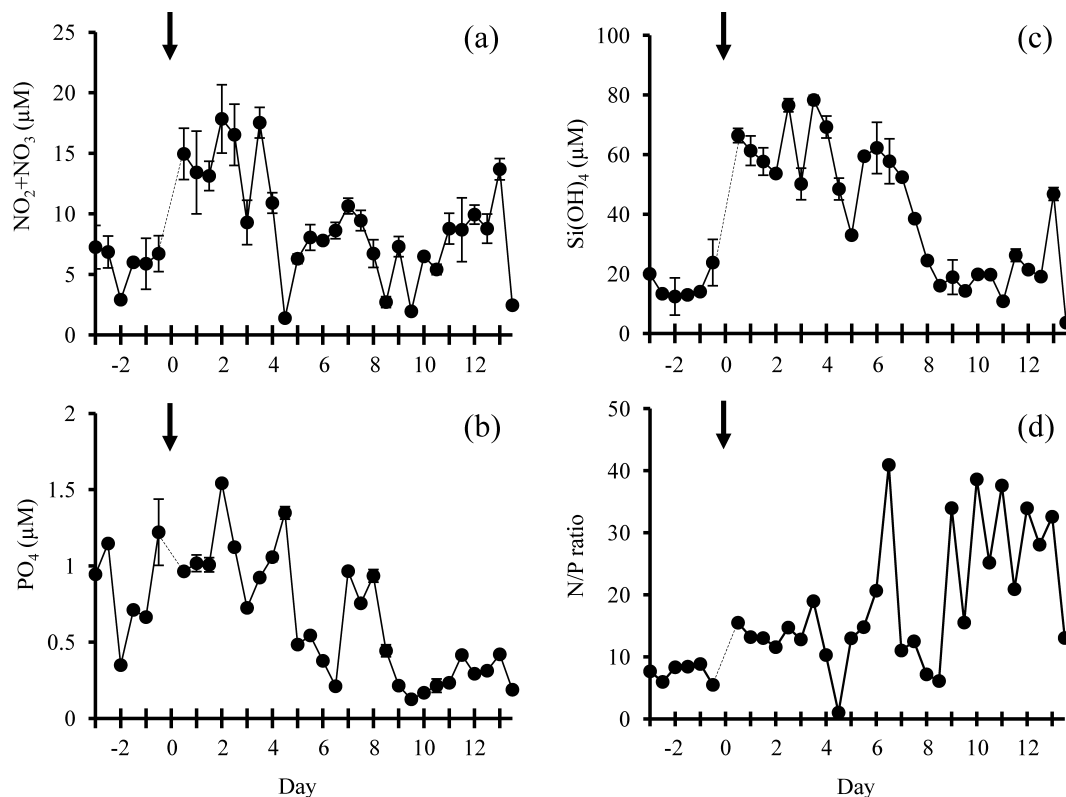


Fig. 4. Temporal variations in (a) NO_2+NO_3 , (b) PO_4 , (c) $\text{Si}(\text{OH})_4$ and (d) N/P ratio at the surface at Sta. A. Arrows show the day of the passage of typhoon *Mawar* in Sagami Bay, Japan. The sampling at 0:00 on Day 0 was interrupted because *Mawar* was closest to the sampling site (dashed line).

Phytoplankton assemblage

Phytoplankton cell abundances exhibited similar fluctuations to chl *a* concentrations (Fig. 6e). Relatively high cell abundances of $8.69 \pm 2.18 \times 10^3$ cells mL^{-1} were observed before the passage of *Mawar* (from Day -3 to Day -1). During that period (before *Mawar*), *Skeletonema* spp. were the most dominant group, representing $85.9 \pm 10.3\%$ of total phytoplankters, followed by *Chaetoceros* spp. ($6.82 \pm 9.42\%$), *Pseudo-nitzschia* spp. ($2.56 \pm 0.48\%$) and *Leptocylindrus* spp. ($1.85 \pm 0.42\%$; Fig. 6f). The cell abundance decreased to $9.22 \pm 6.97 \times 10^2$ cells mL^{-1} on average from Day 0 to Day 2. *Skeletonema* spp. were also the most dominant from Day 0 to Day 3 except for Day 2 when the assemblage was characterized by *Pseudo-nitzschia* spp. being dominant at 31.5%, followed by dinoflagellates at 23.1% and other diatoms such as *Thalassionema nitzschioides* Grunow, *Cylindrotheca closterium* Ehrenberg and *Thalassiosira* spp. at 21.5% of the total cell abundance (Fig. 6f). The cell abundance abruptly increased to the highest value of 1.55×10^4 cells mL^{-1} on Day 5 when the first chl *a* concentration peak was observed (Fig. 6e). *Skeletonema* spp. were also the most dominant at 81.6% on Day 5. Following the first peak, the most dominant taxon changed to *Chaetoceros* spp., which were dominant at $50.6 \pm 4.2\%$ from Day

7 to Day 9 (Fig. 6f). Finally, a peak of *Leptocylindrus* spp. of $54.1 \pm 17.7\%$ ($1.25 \pm 1.39 \times 10^3$ cells mL^{-1}) was observed on Day 10 lasting to Day 13.

According to the MDS analysis, the community structures were categorizable into four significant groups (Group A, B, C and D; analysis of similarities, Global $R=0.892$, $p<0.001$; Fig. 7). The community before the passage of *Mawar* (i.e. Day -3 to Day -1; Group A) was dominated by high cell abundances of *Skeletonema* spp., shifting to Group B, characterized by low cell abundances of *Skeletonema* spp., and then shifting to Group C, characterized by low cell abundances dominated by *Pseudo-nitzschia* spp. and dinoflagellates. From Day 7, the community shifted to Group D which was dominated by *Leptocylindrus* spp.

NO_2+NO_3 , PO_4 and $\text{Si}(\text{OH})_4$ concentrations during the periods of Group B and Group C were relatively high compared to during the periods of Group A and Group D (Fig. 8a, b, c). There were significant differences in NO_2+NO_3 concentrations between Group A and Group B, and in the N/P ratio between Group A and Group D (Scheffe's F multiple comparison, $p<0.05$, Fig. 8a, d). Group C was excluded from the multiple comparison analysis due to the limited number of samples.

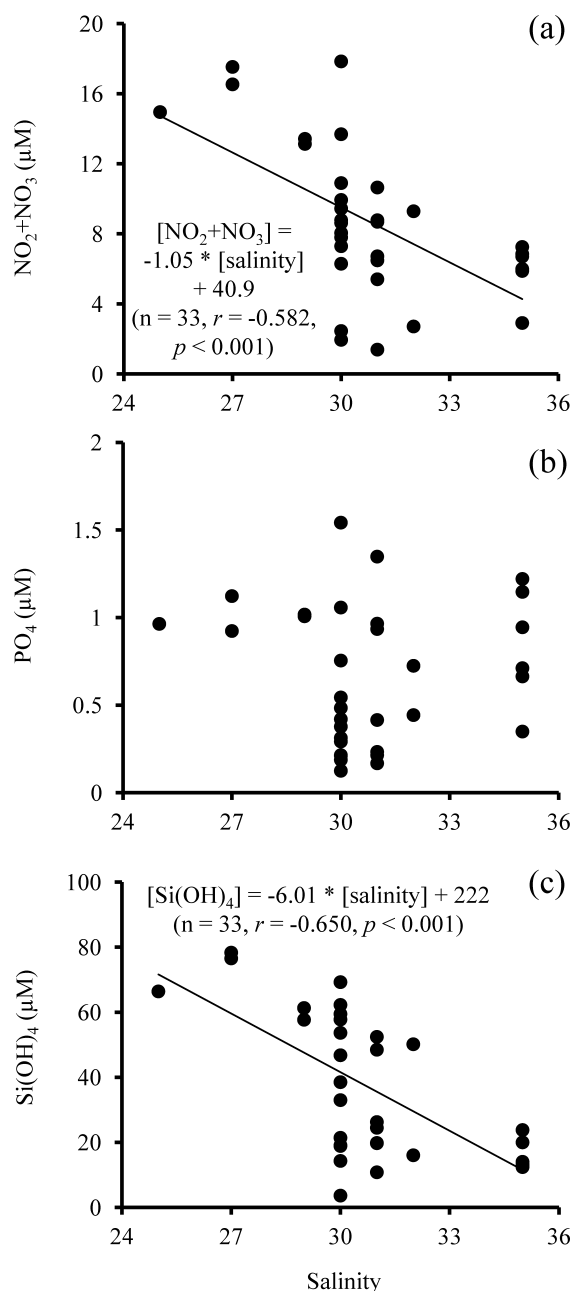


Fig. 5. Relationships between salinity and, (a) NO_2+NO_3 , (b) PO_4 and (c) $\text{Si}(\text{OH})_4$ concentrations.

Discussion

Nutrient origin

Nutrient supply in marine environments is often caused by wind-induced vertical mixing/coastal upwelling (e.g. Shiah et al. 2000), sediment resuspension (e.g. Fogel et al. 1999), terrestrial runoff (e.g. Chen et al. 2009), or a combination of these factors. In the present study, increases in inorganic macronutrient concentrations were observed before the passage of *Mawar*. At the same time, POC concen-

trations increased though chl *a* concentrations and cell abundances did not increase. The increase of POC might have been due to non-phytoplanktonic matter. Because strong winds of 8 m sec^{-1} or more were observed from Day -2 to Day -0.5, sediment resuspension could have been induced and consequently caused the increase in POC concentrations and nutrient elution from sedimentary pore water. In Lake Biwa, PO_4 concentrations and suspended sediment increased after the passage of a typhoon, which implied sedimentary pore water supply of PO_4 to the water column (Robarts et al. 1998). Thus, the increase in inorganic macronutrient concentrations might also be attributable to sediment resuspension during the passage of *Mawar* in the present study.

After *Mawar*, the concentrations of all measured nutrients (NO_2+NO_3 , PO_4 and $\text{Si}(\text{OH})_4$) increased to Day 3.5 (Fig. 4). In Sagami Bay, high concentrations of NO_2+NO_3 and $\text{Si}(\text{OH})_4$ have been observed after heavy rainfall, when the supplies of these nutrients to the coastal regions are related to the increase in freshwater discharge due to precipitation (Fujiki et al. 2004, Baek et al. 2009). Thus, the significant negative relationships between NO_2+NO_3 and $\text{Si}(\text{OH})_4$, and salinity indicate those nutrients were supplied by terrestrial runoff in the present study. In addition, prevailing south winds are known to induce local upwelling off the east coast of the Izu Peninsula (Kishi 1976, 1977). During the passage of *Mawar*, southerly winds were observed at the Ajiro Office, located on the east coast of the Izu Peninsula. According to hydrographic conditions reported by the Kanagawa Prefectural Fisheries Technology Center (<http://www.agri-kanagawa.jp/suisoken/noaa2/noaa2.asp>), a cold water mass, which might have been caused by coastal upwelling, prevailed around the western part of Sagami Bay on Day 2 after the passage of *Mawar*. This suggests that coastal upwelling also supplied NO_2+NO_3 , $\text{Si}(\text{OH})_4$ and PO_4 into the photic zone.

Chl *a* and primary production

Chl *a* exhibited two concentration peaks, on Day 5 and after Day 9.5. The high chl *a* concentration on Day 5 was a result of high primary productivity due to the increase in nutrient concentrations and high PAR following *Mawar*. After the highest chl *a* concentration on Day 5, although a high assimilation number was maintained, the chl *a* concentration decreased. The relative decrease in chl *a* concentration (e.g. Day 5.5, Day 7.5 and Day 8.5) could be due to advection attributable to the ebb tide. High chl *a* concentration after Day 9.5 was the result of the high primary production on Day 9. Relatively high phytoplankton biomass after Day 9.5 might be maintained due to small-scale nutrient loading accompanied by bad weather from Day 10 to Day 12, though primary productivity was low due to low PAR.

Primary production exhibited a relatively low value on Day 1 and was at its maximum on Day 3. Assimilation numbers exhibited high values from Day 1, lasting until

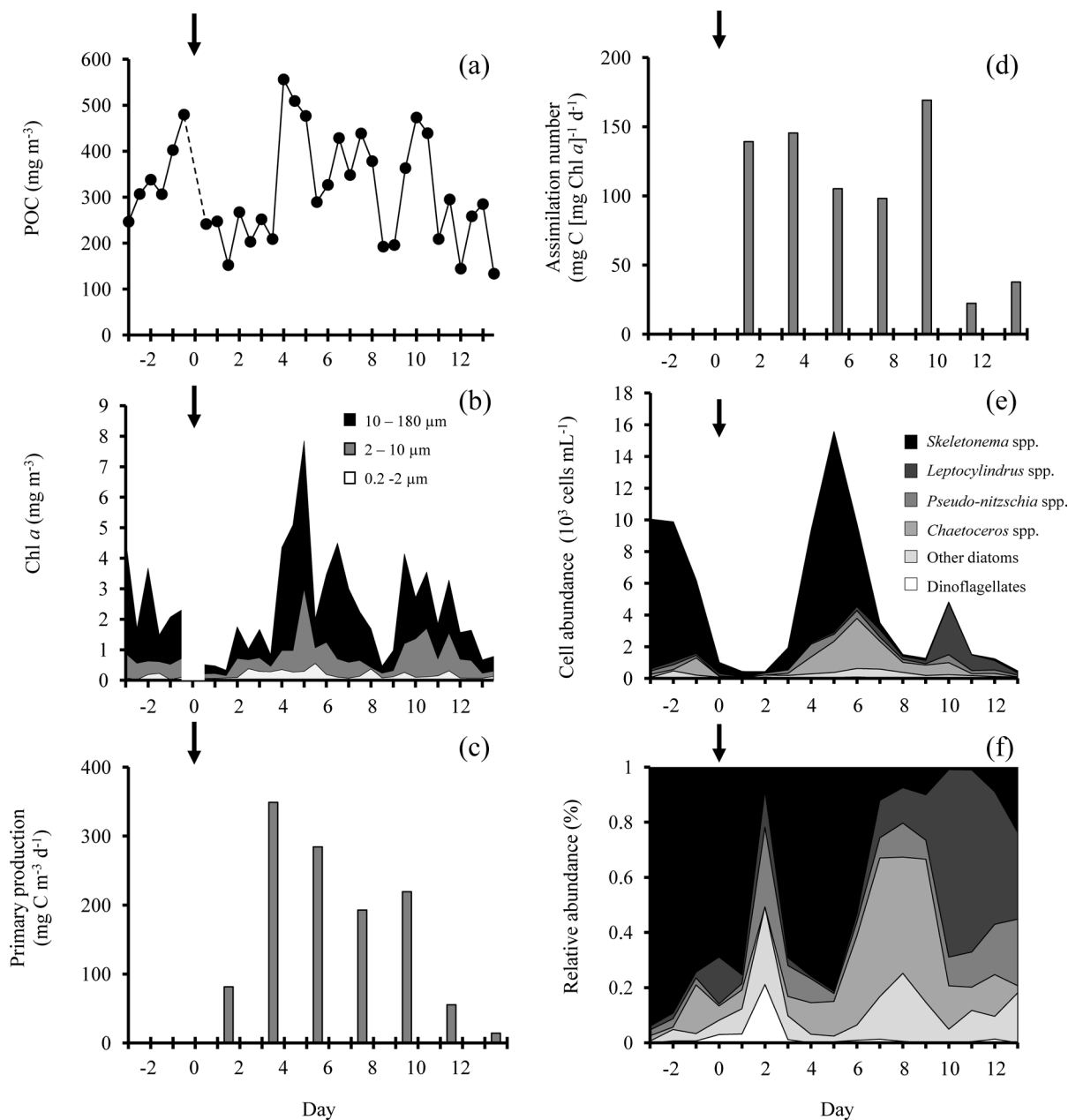


Fig. 6. Temporal variations in (a) particulate organic carbon (POC) concentration, (b) chlorophyll *a* (chl *a*) concentration, (c) primary production, (d) assimilation number, (e) phytoplankton cell abundance and (f) relative abundance of phytoplankton at the surface at Sta. A. Arrows show the day of the passage of typhoon *Mawar* in Sagami Bay, Japan. The sampling at 0:00 on Day 0 was interrupted because *Mawar* was closest to the sampling site (dashed line or blank). Incubation for primary production measurements started at 9:00 for 24 h. Primary production before *Mawar* was not measured. The seawater sample collected on Day 0.5 was used as representative of the phytoplankton assemblage sample at Day 0. Phytoplankton taxa where their mean relative abundance was more than 5% during the study period are shown in (e) and (f).

Day 9 (131 ± 29 mg C [mg Chl *a*]⁻¹ d⁻¹), which was significantly higher than the mean assimilation number, 40 mg C [mg Chl *a*]⁻¹ d⁻¹, observed in August and September in Sagami Bay (Student's *t*-test, $p < 0.01$) reported by Sugawara et al. (2003). Previous studies utilizing remote sensing measurements reported time lags of 3 to 6 days between phytoplankton blooms and their preceding typhoons

(Subrahmanyam et al. 2002, Lin et al. 2003, Walker et al. 2005, Zheng & Tang 2007). In the present study, phytoplankton exhibited high photosynthetic activity from Day 1, due to the high nutrient concentrations and high PAR following the passage of *Mawar*. After Day 9, the assimilation numbers (22 and 38 mg C [mg Chl *a*]⁻¹ d⁻¹) returned to the values close to mean assimilation number (40 mg C

[mg Chl *a*]⁻¹ d⁻¹) reported by Sugawara et al. (2003). The results suggest that the passage of *Mawar* significantly enhanced primary productivity for nine days.

In order to assess the impacts of typhoons on phytoplankton biomass and production, we calculated the ratios of various values in the literature after typhoon passages (A) and either before typhoon passages or the average values during non-typhoon periods (B), expressing them as A/B ratios (Table 1). In coastal regions, the A/B ratios of chl *a* concentration and primary production reported by previous studies were 0.56–12 (3.3 on average) and 1.2–19 (5.2 on average), respectively (Table 1). These mean A/B

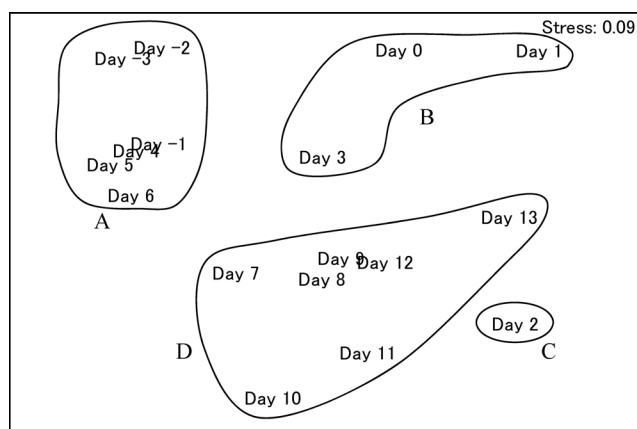


Fig. 7. Multidimensional scaling (MDS) plot of the phytoplankton assemblage at the surface at Sta. A. Four groups, A to D, could be categorized significantly based on an ANOSIM test (Global R=0.892, $p < 0.001$).

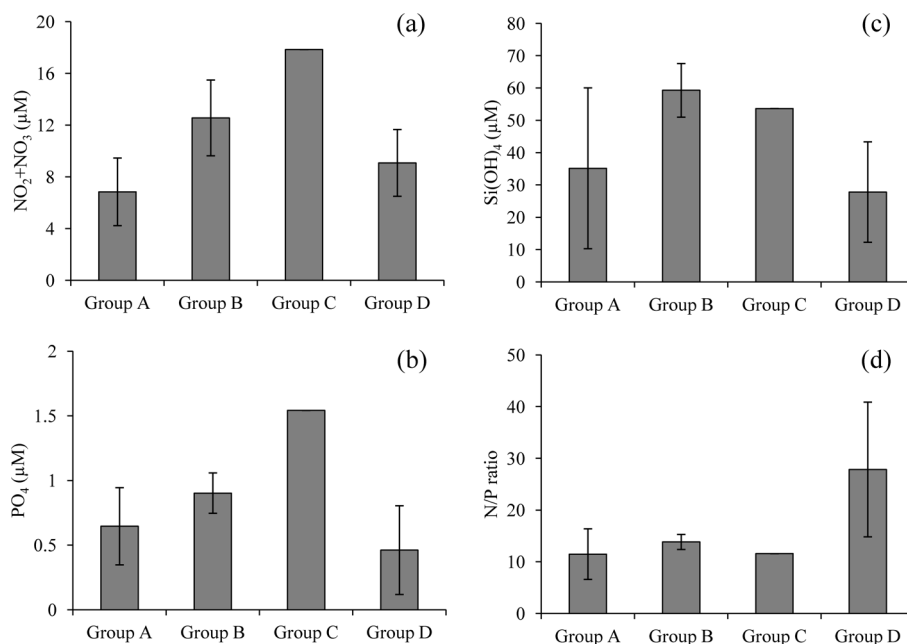


Fig. 8. Mean nutrient status of each phytoplankton assemblage group derived from the Multidimensional Scaling (MDS) analysis (Fig. 7); (a) NO₂+NO₃, (b) PO₄, (c) Si(OH)₄ and (d) N/P ratio.

ratios were similar to the current values of 3.0 for chl *a* concentration and 4.4 for primary production. The A/B ratios tend to vary depending on typhoon and region. Although the A/B ratio data set is scarce, these values could be potential key indices to estimate the effects of typhoons on phytoplankton biomass and production.

The integrated primary production for the nine days after the passage of *Mawar* was 2.10×10^3 mg C m⁻³, which accounts for 7.2–9.1% of the annual primary production in the upper waters of Sagami Bay [annual primary production values were derived from Satoh et al. 2000 (2.92×10^4 mg C m⁻³ yr⁻¹), Sugawara et al. 2003 (2.30×10^4 mg C m⁻³ yr⁻¹) and Ara & Hiromi 2009 (2.82×10^4 mg C m⁻³ yr⁻¹)] (Table 2). In the oceanic region of the South China Sea, integrated primary production at the bloom centre after typhoon passages have been calculated, and accounted for 9.9–23% of the annual primary production derived from Liu et al. (2002) (Lin et al. 2003, Zhao et al. 2008; Table 2). Approximately 3 typhoons on average approach Sagami Bay annually (Japan Meteorological Agency), which implies that primary production in the upper waters of Sagami Bay may be enhanced in the range of 21.6–27.3% of the annual primary production. The present study verified that episodic events such as typhoons can make large contributions to annual primary production in temperate coastal regions.

Phytoplankton assemblages

The increase in chl *a* concentration after the passage of *Mawar* was attributable to larger size phytoplankton, mostly diatoms such as *Skeletonema* spp. and *Leptocylindrus* spp. The response of diatoms in the present study to

Table 2. Summary of contributions of typhoons to annual primary production (PP).

Study site	Typhoon		Enhanced integrated PP	Annual PP*	Contribution %	Reference
	Name	Date				
			mg C m ⁻² (35 d) ⁻¹	mg C m ⁻² yr ⁻¹		
South China Sea	<i>Kai-Tak</i>	Jul-2000	2.96 × 10 ⁴	1.28 × 10 ⁵ ^a	23	Lin et al. 2003
			mg C m ⁻² (20 d) ⁻¹	mg C m ⁻² yr ⁻¹		
South China Sea	<i>Ling-Ling</i>	Nov-2001	1.27 × 10 ⁴	1.28 × 10 ⁵ ^a	9.9	Zhao et al. 2008
South China Sea	<i>Kai-Tak</i>	Oct-2005	1.34 × 10 ⁴	1.28 × 10 ⁵ ^a	10	Zhao et al. 2008
			mg C m ⁻³ (9 d) ⁻¹	mg C m ⁻³ yr ⁻¹		
Sagami Bay	<i>Mawar</i>	Aug-2005	2.10 × 10 ³	2.30–2.92 × 10 ⁴ ^{b,c,d}	7.2–9.1	Present study

Annual PP were derived from (a) Liu et al. (2002), (b) Satoh et al. (2000), (c) Suagawara et al. (2003) and (d) Ara & Hiromi (2009)

*Annual PP was not measured in the same year as when the typhoons occurred

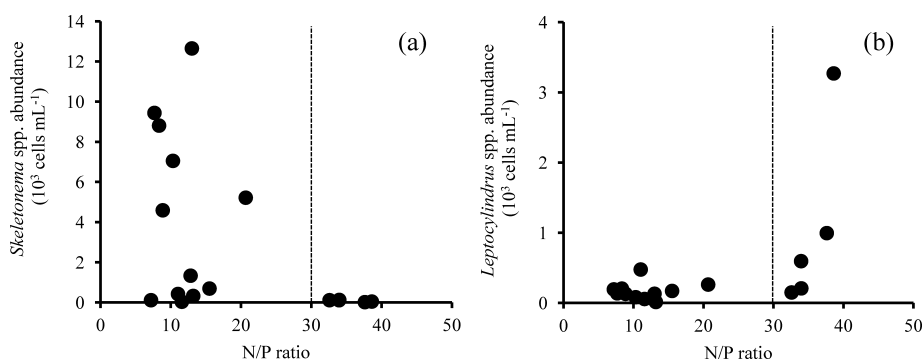


Fig. 9. Relationships between abundance of (a) *Skeletonema* spp. and (b) *Leptocylindrus* spp., and N/P ratio. The dotted line (N/P ratio=30) is derived from Roden & O'Mahony (1984).

typhoon passage is in general agreement with previous studies (Glynn et al. 1964, Zeeman 1985, Furnas 1989, Delesalle et al. 1993, Chang et al. 1996, Chen et al. 2009). *Skeletonema* spp. were dominant after typhoon passage in Puerto Rico (Glynn et al. 1964), South Carolina (Zeeman 1985) and Northern Taiwan (Chang et al. 1996). Other diatoms such as *Chaetoceros* spp., *Nitzschia* spp., *Hemiaulus* spp. and *Rhizosolenia* spp. were also reported dominant after typhoon passages (Zeeman 1985, Furnas 1989, Delesalle et al. 1993, Chen et al. 2009). Larger phytoplankton such as diatoms show higher photosynthetic rates than smaller phytoplankton in eutrophic environments (Cormeño et al. 2005). Diatom biomass subsequently sinks to deeper depths rather than being recycled in the shallow-water food web (Dugdale & Wilkerson 1998, Chen et al. 2009). Thus, typhoon passage may affect the carbon flux and trophic structures in temperate coastal regions as well as subtropical oceanic regions (Chen et al. 2009).

The MDS analysis suggests that the phytoplankton assemblage transitioned through two groups (Group B and

C) just after the passage of *Mawar*, and shifted back to Group A by Day 4. The phytoplankton succession before and after *Mawar* was represented by *Skeletonema* spp. This phytoplankton genus often exhibits euryhaline characteristics (e.g. Brand 1984, Balzano et al. 2011) and a short time-lag between nutrient uptake and growth (e.g. Collos 1986).

In Group A and Group D, which exhibited relatively high chl *a* concentrations, *Skeletonema* spp. and *Leptocylindrus* spp. were the dominant groups, respectively. Although NO₂+NO₃, PO₄ and Si(OH)₄ concentrations exhibited no significant differences between the two groups, the N/P ratios of Group A (11.5±4.9) and Group D (27.9±13.0) were significantly different between the two groups (Student's t-test, *p*<0.05, Fig. 8d). We examined the relationships between the N/P ratio, and abundances of *Skeletonema* spp. and *Leptocylindrus* spp. (Fig. 9a, b). Roden & O'Mahony (1984) conducted an outdoor experiment in an enclosure and reported that *Skeletonema* spp. favor low N/P ratios, and are dominant when the N/P ratio is less

than 30. In the present study, *Skeletonema* spp. cell abundance was significantly higher at an N/P ratio of less than 30 compared to when the N/P ratio was more than 30 (Mann-Whitney U-test, $p < 0.05$, Fig. 9a). On the other hand, *Leptocylindrus* spp. showed the opposite trend, with significantly higher cell abundance at an N/P ratio of more than 30 (Mann-Whitney's U-test, $p < 0.05$, Fig. 9b). The results suggest their respective dominance might be regulated by variations in the N/P ratio.

Prior studies of N/P ratios related to cellular and ambient nutrient status suggest the optimum N/P ratio for *Skeletonema* spp. falls within the range of 8–9 (Parsons et al. 1961, Sakshaug & Olsen 1986, Manabe 1989). The N/P ratios reported after typhoon passages were 9.9 in South Carolina (Zeeman 1985) and 11.5 in northern Taiwan (Chang et al. 1996), which are similar to values found in the present study (12.4) after the typhoon passage when *Skeletonema* spp. were dominant. The range of N/P ratios (9.9–12.4) after the passage of typhoons is similar to levels found in previous studies of *Skeletonema* spp. (Parsons et al. 1961, Roden & O'Mahony 1984, Sakshaug & Olsen 1986, Manabe 1989).

When *Leptocylindrus* spp. increased from Day 9 to Day 10, the PO_4 concentration was $0.17 \pm 0.04 \mu\text{M}$ and the N/P ratio was 29.4 ± 12.2 . Once PO_4 concentrations became low ($< 0.2 \mu\text{M}$) and the N/P ratio increased (> 30), *Leptocylindrus* spp. dominated the phytoplankton assemblage. Similar findings have been reported in microcosm and mesocosm experiments, as well as *in situ* observations. In a microcosm experiment, *Leptocylindrus danicus* Cleve dominated the phytoplankton assemblage during phosphorus-limited conditions, when the N/P ratio was 156.3 (Estrada et al. 2003). In a mesocosm experiment where phosphorus was added, *L. danicus* was dominant under N/P ratios of 29.3, 68.3 and 136.7 (Escaravage et al. 1996). In a coastal region, *Leptocylindrus* spp. dominated when the N/P ratio was 30 or more (Del Amo et al. 1997a, b). In the present study, succession in the phytoplankton assemblage was clearly linked to the variation of the N/P ratio and stoichiometry after the passage of *Mawar*.

Typhoons are important disturbance events occurring near the western boundaries of tropical, subtropical and temperate regions (e.g. Tseng et al. 2010). Dramatic variations in physical and chemical factors occurred during and after the passage of *Mawar*. The bi-daily sampling conducted in the present study revealed the timing, magnitude, and productivity of phytoplankton blooms induced by *Mawar*. The enhanced primary production during the nine days after *Mawar* accounted for up to 9.1% of the annual primary production in the upper waters of Sagami Bay. The succession of the phytoplankton assemblage was closely related to variations in the N/P ratio after *Mawar*. Further studies are needed at multiple sites and depths in order to clarify spatial and temporal variations of physical, chemical and biological factors after the passages of typhoon. Meteorological disturbances such as typhoons,

which will likely intensify as global climate change progresses, should be considered in annual production models.

Acknowledgements

We are grateful to the staff members at Manazuru Marine Center for Environmental Research and Education, Yokohama National University, and Mr. Kenichi Mori, for their cooperation and support in collecting samples. This work was partly supported by Grants-in-Aid for Scientific Research (20780146) of Japan Society for the Promotion of Science.

References

- Ara K, Hiromi J (2009) Seasonal variability in plankton food web structure and trophodynamics in the neritic area of Sagami Bay, Japan. *J Oceanogr* 65: 757–779.
- Ara K, Yamaki K, Wada K, Fukuyama S, Okutsu T, Nagasaka S, Shiomoto A, Hiromi J (2011) Temporal variability in physico-chemical properties, phytoplankton standing crop and primary production for 7 years (2002–2008) in the neritic area of Sagami Bay, Japan. *J Oceanogr* 67: 87–111.
- Baek SH, Shimode S, Kim HC, Han MS, Kikuchi T (2009) Strong bottom-up effects on phytoplankton community caused by a rainfall during spring and summer in Sagami Bay, Japan. *J Mar Syst* 75: 253–264.
- Balzano S, Sarno D, Kooistra WHCF (2011) Effects of salinity on the growth rate and morphology of ten *Skeletonema* strains. *J Plankton Res* 33: 937–945.
- Behrenfeld MJ, Falkowski PG (1997) Photosynthetic rates derived from satellite-based chlorophyll concentration. *Limnol Oceanogr* 42: 1–20.
- Brand LE (1984) The salinity tolerance of forty-six marine phytoplankton isolates. *Estuar Coast Shelf Sci* 18: 543–556.
- Cermeño P, Marañón E, Rodríguez J, Fernández E (2005) Large-sized phytoplankton sustain higher carbon-specific photosynthesis than smaller cells in a coastal eutrophic ecosystem. *Mar Ecol Prog Ser* 297: 51–60.
- Chang J, Chung C, Gong G (1996) Influences of cyclones on chlorophyll *a* concentration and *Synechococcus* abundance in a subtropical western Pacific coastal ecosystem. *Mar Ecol Prog Ser* 140: 199–205.
- Chen YL, Chen H, Jan S, Tuo S (2009) Phytoplankton productivity enhancement and assemblage change in the upstream Kuroshio after typhoons. *Mar Ecol Prog Ser* 385: 111–126.
- Chihara M, Fukuyo Y, Inoue H, Takayama H, Horiguchi T, Matsuoka K, Toriumi S, Kawachi M, Hara H, Takano H (1997) Division Dinophyta and Division Heterokontophyta. In: An illustrated guide to marine plankton in Japan (eds Chihara M., Murano M). Tokai University Press, Tokyo, pp. 31–260. (in Japanese)
- Collos Y (1986) Time-lag algal growth dynamics: biological constraints on primary production in aquatic environments. *Mar Ecol Prog Ser* 33: 193–206.
- Del Amo Y, Le Pape O, Tréguer P, Quéguiner B, Ménesguen A, Aminot A (1997a) Impacts of high-nitrate freshwater inputs on

- macrotidal ecosystems. I. Seasonal evolution of nutrient limitation for the diatom-dominated phytoplankton of the Bay of Brest (France). *Mar Ecol Prog Ser* 161: 213–224.
- Del Amo Y, Quéguiner B, Tréguer P, Breton H, Lampert L (1997b) Impacts of high-nitrate freshwater inputs on macrotidal ecosystems. II. Specific role of the silicic acid pump in the year-round dominance of diatoms in the Bay of Brest (France). *Mar Ecol Prog Ser* 161: 225–237.
- Delesalle B, Pichon M, Frankignoulle M, Gattuso PJ (1993) Effects of a cyclone on coral reef phytoplankton biomass, primary production and composition (Moorea Island, French Polynesia). *J Plankton Res* 15: 1413–1423.
- Dugdale RC, Wilkerson FP (1998) Silicate regulation of new production in the equatorial Pacific upwelling. *Nature* 391: 270–273.
- Emanuel K (2005) Increasing destructiveness of tropical cyclones over the past 30 years. *Nature* 436: 686–688.
- Elsner BJ, Kossin PJ, Jagger HT (2008) The increasing intensity of the strongest tropical cyclones. *Nature* 455: 92–95.
- Escaravage V, Prins TC, Smaal AC, Peethers JCH (1996) The response of phytoplankton communities to phosphorus input reduction in mesocosm experiments. *J Exp Mar Biol Ecol* 198: 55–79.
- Estrada M, Berdalet E, Vila M, Marrase C (2003) Effects of pulsed nutrient enrichment on enclosed phytoplankton: eco-physiological and successional responses. *Aquat Microb Ecol* 32: 61–71.
- Fogel ML, Aguilar C, Cuhel R, Hollander DJ, Willey JD, Paerl HW (1999) Biological and isotopic changes in coastal waters induced by Hurricane Gordon. *Limnol Oceanogr* 44: 1359–1369.
- Fujiki T, Toda T, Kikuchi T, Aono H, Taguchi S (2004) Phosphorus limitation of primary productivity during the spring–summer blooms in Sagami Bay, Japan. *Mar Ecol Prog Ser* 283: 29–38.
- Fukuyo Y, Horiguchi T, Katsuhisa Y, Yoshimatsu S, Takayama H, Matsuoka K, Toriumi S, Ono C, Kuroda K, Inoue H, Pholpunthin P, Imamura K, Takano H (1990) III. Dinophyceae and IV. Bacillariophyceae. In: *Red tide organisms in Japan: an illustrated taxonomic guide* (eds Fukuyo Y, Chihara M, Takano H, Matsuoka K). Uchida-Roukakuho, Tokyo, pp. 22–331. (in Japanese)
- Furnas MJ (1989) Cyclonic disturbance and a phytoplankton bloom in a tropical shelf ecosystem. In: *Red Tides: Biology, Environmental Science and Toxicology* (eds Okaichi T, Anderson DM, Nemoto T). Elsevier, New York, pp. 273–276.
- Furnas MJ (1990) *In situ* growth rates of marine phytoplankton: approaches to measurement, community and species growth rates. *J Plankton Res* 12: 1117–1151.
- Gao K, McKinley KR (1994) Use of macroalgae for marine biomass production and CO₂ remediation: a review. *J Appl Phycol* 6: 45–60.
- Glynn PW, Almodovar LR, Gonzalez JG (1964) Effects of hurricane Edith on marine life in La Parguera, Puerto Rico. *Caribb J Sci* 4: 335–345.
- Hama T, Miyazaki Y, Ogawa Y, Iwakuma T, Takahashi M, Otsuki A, Ichimura S (1983) Measurement of photosynthetic production of a marine phytoplankton population using a stable ¹³C isotope. *Mar Biol* 73: 31–36.
- Hashimoto N, Yamaguchi Y, Ishimaru T, Saino T (2005) Relationship between net and gross primary production in the Sagami Bay, Japan. *Limnol Oceanogr* 50: 1830–1835.
- Hasle RG (1978) The inverted microscope method. In: *Monographs on oceanographic methodology*, Vol 6, Phytoplankton manual (ed Sournia A). UNESCO, Paris, pp. 88–96.
- Hasle RG, Syvertsen EE (1997) Chapter 2. Marine Diatoms. In: *Identifying marine phytoplankton* (ed Tomas RC). Academic Press, San Diego, pp. 5–386.
- Hirano T (1969) Investigation of the impact of river water withdrawal on fisheries. Agricultural Policy Planning Department, Kanagawa Prefecture, pp. 9–13. (in Japanese)
- Hogetsu K, Taga N (1977) Suruga Bay and Sagami Bay. In: *JIBP Synthesis, Productivity of Biocenoses in Coastal Regions of Japan*, Vol. 14 (eds Hogetsu K, Hatanaka M, Hanaoka T, Kawamura T). University of Tokyo Press, Tokyo, pp. 31–172.
- Holm-Hansen O, Lorenzen CJ, Holmes RN, Strickland JDH (1965) Fluorometric determination of chlorophyll. *J Cons Perm Int Explor Mer* 30: 3–15.
- Horikoshi M (1977) Suruga Bay and Sagami Bay. In: *JIBP Synthesis, Productivity of Biocenoses in Coastal Regions of Japan*, Vol. 14 (eds Hogetsu K, Hatanaka M, Hanaoka T, Kawamura T). University of Tokyo Press, Tokyo, pp. 62–69.
- Hydrographic Department, Japan Coast Guard (1992) *Tidal Harmonic Constants Tables*. In: *Bibliography No. 742* (ed Hydrographic Department, Japan Coast Guard). Japan Hydrographic Association, Tokyo. (in Japanese)
- Japan Meteorological Agency (2011) *Meteorological Data Acquisition System (AMeDAS)*. Available at: <http://www.jma.go.jp/> (accessed on 10 August 2011)
- Japan Meteorological Agency (2011) *Tropical Cyclone Information*. Available at: <http://www.jma.go.jp/jp/typh/> (accessed on 10 August 2011)
- Jickells TD (1998) Nutrient biogeochemistry of the coastal zone. *Science* 281: 217–222.
- Kanagawa Prefectural Fisheries Technology Center (2012) *Hydrographic condition report*. Available at: <http://www.agrikanagawa.jp/suisoken/noaa2/noaa2.asp> (accessed on 1 September 2012)
- Kanda J, Fujiwara S, Kitazato H, Okada Y (2003) Seasonal and annual variation in the primary production regime in the central part of Sagami Bay. *Prog Oceanogr* 57: 17–29.
- Kishi M (1976) Upwelling along the east coast of the Izu Peninsula (I). *Umi to Sora* 51: 105–113.
- Kishi M (1977) Upwelling along the east coast of the Izu Peninsula (II). *Umi to Sora* 52: 59–65.
- Kitazato H, Shirayama Y, Nakatsuka T, Fujiwara S, Shimanaga M, Kato Y, Okada Y, Kanda J, Yamaoka A, Masuzawa T, Suzuki K (2000) Seasonal phytodetritus deposition and responses of bathyal benthic foraminiferal populations in Sagami Bay, Japan: preliminary results from “Project Sagami 1996–1999”. *Mar Micropaleontol* 40: 135–149.
- Kuwahara VS, Ogawa H, Toda T, Kikuchi T, Taguchi S (2000a) Variability in the relative penetration of ultraviolet radiation to photosynthetically available radiation in temperate coastal waters, Japan. *J Oceanogr* 56: 399–408.
- Kuwahara VS, Ogawa H, Toda T, Kikuchi T, Taguchi S (2000b)

- Variability of bio-optical factors influencing the seasonal attenuation of ultraviolet radiation in temperate coastal waters of Japan. *Photochem Photobiol* 72: 193–199.
- Lagus A, Suomela J, Weithoff G, Heikkila K, Helminen H, Siipura J (2004) Species-specific differences in phytoplankton responses to N and P enrichments and the N:P ratio in the Archipelago Sea, northern Baltic Sea. *J Plankton Res* 26: 779–798.
- Lin I, Liu WT, Wu C, Wong GTF, Hu C, Chen Z, Liang W, Yang Y, Liu K (2003) New evidence for enhanced ocean primary production triggered by tropical cyclone. *Geophys Res Lett* 30: 1718, doi:10.1029/2003GL017141.
- Liu K, Chao S, Shaw P, Gong G, Chen C, Tang, T (2002) Monsoon-forced chlorophyll distribution and primary production in the South China Sea: observations and a numerical study. *Deep-Sea Res Part I* 49: 1387–1412.
- Manabe T (1989) Elemental composition of *Skeletonema costatum* and proposed theoretical chemical formula. *Bull Plankton Soc Japan* 36: 43–46. (in Japanese with English abstract)
- Miyaguchi H, Kurosawa N, Toda T (2008) Real-time polymerase chain reaction assays for rapid detection and quantification of *Noctiluca scintillans* zoospore. *Mar Biotechnol* 10: 133–140.
- Nakata N (1985) Sagami Bay: Biology. In: Coastal oceanography of Japanese Islands (ed Oceanographical Society of Japan). Tokai University Press, Tokyo, pp. 417–427. (in Japanese)
- Nagao N, Toda T, Takahashi K, Hamasaki K, Kikuchi T, Taguchi S (2001) High ash content in net-plankton samples from shallow coastal water: possible source of error in dry weight measurement of zooplankton biomass. *J Oceanogr* 57: 105–107.
- Ogura F (1975) Further studies on decomposition of dissolved organic matter in coastal seawater. *Mar Biol* 31: 101–111.
- Paerl HW (1995) Coastal eutrophication in relation to atmospheric nitrogen deposition: current perspectives. *Ophelia* 41: 237–259.
- Parsons TR, Stephens K, Strickland JDH (1961) On the chemical composition of eleven species of marine phytoplankton. *J Fish Res Bd Canada* 18: 1001–1016.
- Parsons TR, Maita Y, Lalli CM (1984) A manual of chemical and biological methods for seawater analysis. Pergamon Press, Oxford, 173 pp.
- Price JF (1981) Upper ocean response to a hurricane. *J Phys Oceanogr* 11: 153–175.
- Roberts RD, Waiser MJ, Hadas O, Zohary T, MacIntyre S (1998) Relaxation of phosphorus limitation due to typhoon-induced mixing in two morphologically distinct basins of Lake Biwa, Japan. *Limnol Oceanogr* 43: 1023–1036.
- Roden CM, O'Mahony KW (1984) Competition as a mechanism of adaptation to environmental stress in outdoor cultures of marine diatoms. *Mar Ecol Prog Ser* 16: 219–227.
- Sakshaug E, Olsen Y (1986) Nutrient status of phytoplankton blooms in Norwegian waters and algal strategies for nutrient competition. *Can Bull Fish Aquat Sci* 43: 389–396.
- Satoh F, Hamasaki K, Toda T, Taguchi S (2000) Summer phytoplankton bloom in Manazuru Harbor, Sagami Bay, central Japan. *Plankton Biol Ecol* 47: 73–79.
- Shiah FK, Chung SW, Kao SJ, Gong GC, Liu KK (2000) Biological and hydrographical responses to tropical cyclones (typhoons) in the continental shelf of the Taiwan Strait. *Cont Shelf Res* 20: 2029–2044.
- Sieburth JMcN, Smetacek V, Thorarinsson F (1978) Pelagic ecosystem structure: Heterotrophic compartments of plankton and their relationship to plankton size fractions. *Limnol Oceanogr* 23: 1256–1263.
- Subrahmanyam B, Rao KH, Rao NS, Murty VSN, Sharp RJ (2002) Influence of a tropical cyclone on chlorophyll *a* concentration in the Arabian Sea. *Geophys Res Lett* 29: 2065, doi:10.1029/2002GL015892.
- Sugawara T, Hamasaki K, Toda T, Kikuchi T, Taguchi S (2003) Response of natural phytoplankton assemblages to solar ultraviolet radiation (UV-B) in the coastal water, Japan. *Hydrobiologia* 493: 17–26.
- Sun L, Yang Y, Xian T, Lu Z, Fu Y (2010) Strong enhancement of chlorophyll *a* concentration by a weak typhoon. *Mar Ecol Prog Ser* 404: 39–50.
- Suzuki R, Ishimaru T (1990) An improved method of the determination of phytoplankton chlorophyll using *N, N*-Dimethylformamide. *J Oceanogr* 46: 190–194.
- Tseng YF, Hsu TC, Chen YL, Kao SJ, Wu JT, Lu JC, Lai CC, Kuo HY, Lin CH, Yamamoto Y, Xiao T, Shiah FK (2010) Typhoon effects on DOC dynamics in a phosphate-limited reservoir. *Aquat Microb Ecol* 60: 247–260.
- Yamada Y, Oouchi K, Satoh M, Tomita H, Yanase W (2010) Projection of changes in tropical cyclone activity and cloud height due to greenhouse warming: Global cloud-system-resolving approach. *Geophys Res Lett* 37: L07709, doi:10.1029/2010GL042518.
- Walker ND, Leben RR, Balasubramanian S (2005) Hurricane-forced upwelling and chlorophyll *a* enhancement within cold-core cyclones in the Gulf of Mexico. *Geophys Res Lett* 32: L18610, doi:10.1029/2005GL023716.
- Webster PJ, Holland GJ, Curry JA, Chang HR (2005) Changes in tropical cyclone number, duration, and intensity in a warming environment. *Science* 309: 1844–1846.
- Zeeman IS (1985) The effects of tropical storm Dennis on coastal phytoplankton. *Estuar Coast Shelf Sci* 20: 403–418.
- Zhao H, Tang D, Wang Y (2008) Comparison of phytoplankton blooms triggered by two typhoons with different intensities and translation speeds in the South China Sea. *Mar Ecol Prog Ser* 365: 57–65.
- Zheng MG, Tang D (2007) Offshore and nearshore chlorophyll increases induced by typhoon winds and subsequent terrestrial rainwater runoff. *Mar Ecol Prog Ser* 333: 61–74.